KEK Report 88- 8
November 1988
A

Injection of 1 GeV H^- Beam into the JHF I-A Ring

Isao YAMANE, Kiyoshi KITAGAWA, Hirohiko SOMEYA
and Yoshiharu YANO

NATIONAL LABORATORY FOR
HIGH ENERGY PHYSICS

KEK Reports are available from:

Technical Information Office
National Laboratory for High Energy Physics
1-1 Oho, Tsukuba-shi
Ibaraki-ken, 305
JAPAN

Phone: 0298-64-1171
Telex 3652-534 (Domestic)
(0)3652-534 (International)
Cable: KEKOHO

Injection of 1 GeV H^- Beam into the JHF I-A Ring

Isao YAMANE, Kiyoshi KITAGAWA, Hirohiko SOMEYA and Yoshiharu YANO

KEK, National Laboratory for High Energy Physics
1-1 Oho, Tsukuba-shi, Ibaraki-ken, 305, Japan

Abstract

Application of the H^0 injection method to the injection system of the JHF I-A ring was studied. It turned out that the H^0 injection method is adequate when some conditions are fulfilled. The ways to fulfill those conditions are described.

1. Introduction

This is a design study report on the injection system of the JHF (Japan Hadron Facility) I-A ring [1]. The I-A ring is a compressor / stretcher ring with 16 FODO cells. Its plan view and optical parameters of a single cell are shown in Fig.1 and Fig.2, respectively. (See Appendix I, Outline of the I-A Ring) In the plan 1 GeV H^- beam from a linac is injected into the I-A ring. The main parameters of the I-A ring and the 1 GeV H^- beam are listed in Table 1 and Table 2, respectively.

The beam energy of 1 GeV is higher than the highest energy that has ever been used for H^- charge-exchange injection into a synchrotron (800 MeV at PSR). At such a high energy, one of the most important phenomena with respect to the transport of H^- beam is the Lorentz stripping [2], [3]. When a high energy H^- ion traverses a high magnetic field, the second electron, that is weakly bound with 0.755 eV binding energy, is stochastically detached due to the action of the Lorentz force, and the H^- ion is converted to an H^0 atom. (See Appendix II, Lorentz Stripping) This phenomenon usually puts restrictions on the transport line of a high energy H^- beam. But it can also be a very useful technique, using a stripping magnet to produce an H^0 beam [4],[5].

One of the main features of the I-A ring is a very high average current. At such a high average current, even a very small beam loss fraction can make a very high radioactivity around the ring, thus limiting the beam current in routine operation, if "hands-on" maintenance is required. Reduction of the beam loss is an important subject of design study. We aim to suppress beam loss to less than 10^{-3} of the beam current,

expecting that the residual radioactivity will be at about same level as the KEK PS-Booster or lower. And for this reason we chose the H° injection method rather than the direct H^- injection method. (See Appendix III, Direct H^- Injection into the I-A Ring)

At the Los Alamos PSR, 800 MeV H^- beam was injected by the H° injection method, in which H^- beam was first converted to H° beam in a stripping magnet outside the ring and then H° beam was injected to the stripping foil in the ring through a ring bending-magnet.[6] Recent reports on the PSR [7],[8] state that the residual radioactivity reaches an unallowable level at about one third of the design average current. Their explanation is that the high residual radioactivity is produced by beam loss due to a large emittance growth accumulating from angular enlargement in the stripping magnet, mismatch of the H° beam to the ring beam optics and scattering in the stripping foil.

However, 1 GeV of the H^- beam should basically be a most suitable energy for the H° injection method. As the energy of the H^- beam becomes higher, usable magnetic field for the beam handling conversely becomes lower due to the Lorentz stripping, and the size of the magnet becomes larger. On the other hand, when the energy of the H^- beam becomes lower, efficiency of the magnetic stripping rapidly decreases and the angular spread of the H° beam becomes larger. At 1 GeV, neither of these problems are serious. If it is practical, the H° injection method has a very large advantage that it makes the injection system very simple. It seems very important to study whether we can avoid the difficulties that the PSR encountered. Therefore, we studied how to apply the H° injection method to the injection system of the I-A ring.

2. Application of the H° injection method to the I-A ring

2-1 Injection plane and gap direction of the stripping magnet

As is described in the section 3, it is safely expected that the enlargement of angular spread is 0.5 mrad in a stripping magnet; namely a perfectly collimated beam of 1 GeV H^- ions receives an angular spread such that 95 % of the output H° beam is contained between ± 0.5 mrad. This spread enlarges the angular width of the actual H° beam, making it desirable to reduce the distance between the stripping magnet and the stripping foil, to keep the H° beam size from becoming too large at the foil. In the I-A ring, as is shown in Fig. 3, the distance is the smallest (about 3.8 m) when the stripping magnet is set just in front of a ring bending magnet and the stripping foil between the bending magnet and the next quadrupole magnet.

Selection of the injection plane is related to two aperture requirements. One is that the stripping foil should be placed outside the ring acceptance. The other is that the acceptance of 120 π mm-mrad should be guaranteed on the injection bump orbit. In the vertical plane, the wall of the vacuum chamber could not be separated enough from the

boundary of the ring acceptance in the bending magnet, because it is limited by the gap of the magnet. When the stripping foil is set just outside the ring acceptance, it is impossible to satisfy the second requirement. Therefore we selected the horizontal plane for injection and set the stripping foil just outside the horizontal ring-acceptance. Then the polarity of the next quadrupole magnet should be focusing in the horizontal plane, otherwise the injection bump orbit will be more pushed out and more aperture will be needed. At the foil location the horizontal beta function of the ring becomes about maximum and the vertical beta function about minimum because the quadrupole magnet neighbouring to the foil must be focusing in the horizontal plane. Both for reducing the foil-hitting probability of the beam and also for the phase-space painting, it is desirable that the plane in which the beam emittance is left small by the stripping magnet coincide with the plane in which the ring beam becomes larger at the foil. Thus we selected the gap direction of the stripping magnet as horizontal and the median plane as vertical.

2-2 Beam formation in the horizontal plane

In order to pass the beam through the narrow gap of the stripping magnet, it is necessary to make a small waist at the gap. It is also desirable to make the size of the H^0 beam as small as possible at the stripping foil, not only for reducing the foil-hitting probability of beam particles but also for painting the phase space of the ring beam. So we searched for the condition that the beam size at the foil becomes the minimum for the beam forming a waist at the stripping magnet. The process is shown in Fig. 4. As is shown, the half size of such a beam is 3.3 mm at the foil and 2.3 mm at the stripping magnet. It is small enough to pass the stripping magnet gap of at least 11 mm. Parameters of the obtained beam are listed in Table 3. Fitting of emittance ellipse of the H^0 beam to that of the ring beam at the foil is shown in Fig. 6(a).

2-3 Beam formation in the vertical plane

In the vertical plane including the median plane of the stripping magnet, the envelope of phase-space distribution will vary in the following way. Provided the envelope of the injected H^- beam is an ellipse as shown in Fig. 5, it will be deformed to the dotted line by enlargement of the angular spread in the stripping magnet. As a result, the emittance of the beam is also enlarged. Furthermore, it will incline in the drift space between the stripping magnet and the stripping foil, and become such a form as the dashed line. Thus the shape of the envelope is not an ellipse at the foil.

On designing the H^0 beam in the vertical plane, we searched parameters to form a small beam that was nearly a waist and also well fitted to the emittance ellipse of the ring beam at the foil. This search was done by varying parameters of the injected H^- beam with a condition that the point (in left upper of Fig. 5) with the maximum angle on the phase-space envelope came on the axis of angle at the foil. The obtained beam phase-

space envelopes are shown at the right bottom of Fig. 5. Beam parameters are summarized in Table 3 and H^o beam phase-space distribution fitting to the ring beam emittance ellipse is shown in Fig. 6(b). The injected H^- beam does not form a waist but is converging in the stripping magnet.

2-4 Position of the bump magnets

Suppose that we inject a beam into a foil placed at a point of a bump orbit that is formed by a bump magnet pair as is shown in Fig. 7(a), and that the emittance ellipse of the beam to be formed in the ring and the injected beam phase-space envelope are such as shown in Fig. 7(b) at the foil. Then in order to distribute the injected beam over the ring beam emittance ellipse, the bump orbit must be moved between the points P and O. (We will discuss in another section how to move the bump orbit for the phase-space painting.) P is the center of the injected beam phase-space distribution whose envelope contacts the emittance ellipse of the ring beam at the outermost point. O is the emittance ellipse center at the end of the injection. To make the foil-hitting probability minimum, it is desirable to inject the beam at P, and to move the bump orbit from P to O monotonously. When the emittance of the injected beam is negligibly small, this corresponds to the relation

$$\alpha x + \beta x' = 0 \quad . \tag{1}$$

However, when the emittance has a small but unnegligible magnitude, P often comes considerably off the line (1). In such a case, we need a new condition to define the position of the bump magnet B1. This condition is

$$\tan\Delta\psi = \frac{x}{\beta\Delta x'} \quad . \tag{2}$$

(2) is the general condition that is applicable in any case. (1) is a special case of (2) in which $\Delta\psi = 90°$.

As is shown in Fig. 6, $\Delta\psi_x = 87.5°$ for the horizontal plane and $\Delta\psi_y = 112.0°$ for the vertical plane. The resulting bump orbits are shown in Fig. 8 (horizontal) and in Fig. 9 (vertical). The bump orbit in the horizontal plane is pushed out to pass the stripping foil that is placed outside the ring acceptance boundary. Of cource we prepare an acceptance of 120 πmm·mrad for the beam on the bump orbit at the end of injection.

Another report in the reference [1] covers the bump magnets and their power supplies.

2.5 Measures to tune variation

The tune of the ring is expected to be varied more or less for various purposes. When the tune is varied, the phase advance between two bump magnets becomes different from 180° and the bump orbit fails to close. On the other hand, even if the tune is varied, the condition to inject the H° beam into the ring beam emittance ellipse is not changed. Therefore, the part of the bump orbit involving the foil should not be changed. In order to satisfy this requirement, two more bump magnets are installed upstream and downstream of the foil for each plane. Thus the total arrangement of the H° injection system becomes such as shown in Fig. 10.

3. Stripping magnet

3.1 Angular distribution $g(\theta)$ of the output H° beam

If the magnetic field in the stripping magnet is given as a function of length along the beam path, the angular distribution of the output H° beam is calculated as follows. Suppose $B \equiv B(s)$; then we can transform B(s) to a function $B(\theta)$ of deflection angle θ by the relation $B \cdot ds = (B\rho) \cdot d\theta$, where $(B\rho)$ is the magnetic rigidity of H^- ions. Using this function and eq. (A-4), the H^- fraction can be expressed as a function of θ as

$$f(\theta) = \exp\left[-\frac{(B\rho)}{A_1}\int_0^{\theta} \exp\left(\frac{-A_2}{\gamma\beta c B(\xi)}\right) d\xi\right] \qquad (3)$$

Then, the angular distribution $g(\theta)$ of the H° beam made from a perfectly collimated H^- beam is derived as $g(\theta) = -df(\theta)/d\theta$, that is

$$g(\theta) = \frac{(B\rho)}{A_1} \exp\left(\frac{-A_2}{\gamma\beta c B(\theta)}\right) \exp\left[-\frac{(B\rho)}{A_1}\int_0^{\theta} \exp\left(\frac{-A_2}{\gamma\beta c B(\xi)}\right) d\xi\right] . \qquad (4)$$

Calculations using model functions of B(s) show that almost all of 1 GeV H^- beam is stripped in a region where B(s) rises from 0.7 T to 1.6 T, and the width of angular distribution depends on the gradient of B(s) in the region. Examples of calculated angular distribution are shown in Fig. 11. In order to make the 95 % half width (that contains 95 % of the H° beam) 0.5 mrad or smaller, the stripping magnet field gradient should be higher than 1.3 T/cm over the region including 0.7 T and 1.6 T.

3.2 Stripping magnet

In order to generate such a high field gradient as mentioned above, the stripping magnet has a special shape, as is shown in Fig. 12(a). This type of stripping magnet

was first designed at LASL [4]. It has two gaps. One is the main gap and generates a very high field not lower than 1.8 T. The other is the auxiliary gap and generates a field lower than 0.4 T with opposite sign to the field in the main gap. To generate such a high field as 1.8 T, the height of the main gap is made as short as possible, and the poles are made of a special magnetic material with a very high saturation-flux-density. Because at least 10 mm is needed to pass the H^0 beam waist, the gap height becomes no less than 11 mm including the vacuum chamber walls. Furthermore, in order to make the field gradient as high as possible, the distance between the main and the auxiliary poles should be set somewhat shorter than the main gap. In such a design we can safely expect a maximum field no less than 2 T and a field gradient higher than 1.8 T/cm. Fig. 12(b) shows an example of the field distribution calculated with a computer for the pole shape of Fig. 12(a). It suggests that a very high field and also a very high field gradient can be generated when the main poles are made of a proper material and the exciting current is sufficiently high. As the expectable maximum field is higher than 1.8 T and the expectable field gradient is also higher than 1.3 T/cm, it can be safely expected that the 95 % half width will be no more than 0.5 mrad.

4. Stripping foil

4-1 Foil material and thickness

The stripping foil for the H^--charge-exchange injection into a synchrotron is usually a carbon foil when the injection energy is higher than 200 MeV. Also in our case of the I-A ring, a carbon foil is considered to be the best for several reasons. Carbon is the lightest element that is easily formed to a foil; carbon foil has the highest heat resistivity; handling of carbon foils is very easy; and so on.

Factors that should be considered to define the stripping foil thickness are energy loss, emittance growth due to multiple scattering and stripping efficiency. The stopping power [10] of carbon foil against 1 GeV protons is

$$\frac{dE}{dx} = 1.98 \quad (\mathrm{MeV \cdot cm^2/g}) \quad . \tag{5}$$

The foil-hitting probability of the beam during the injection can be made as low as 10 %, as is described in the section of phase-space painting. So a proton will pass the foil at most 60 times. Then the energy loss by a carbon foil of 250 $\mu g/cm^2$ in thickness is at most 30 keV. This is 3×10^{-5} of the beam energy and negligibly small. Even if the thickness of the foil is increased by twice, the situation is not changed.

The emittance growth due to the multiple scattering can be estimated by the formula [11]

$$\Delta\varepsilon = \frac{1}{2}\pi\beta_0 Nnt\,\sigma_c\,\overline{(\delta y')^2} \quad , \tag{6}$$

where β_0 is the beta function at the foil location, N number of passages through the foil, nt is the foil thickness in number of atoms per unit area and

$$\sigma_c\,\overline{(\delta y')^2} = \frac{\pi}{2}\left(\frac{Zr_pE_0}{T}\right)\left[\ln\frac{(\delta\theta_M)_{ch}^2}{\chi_\gamma^2} - 1\right] \quad ,$$

where Z is the charge of the foil atom, r_p the classical radius of proton (= 1.5×10^{-18} m), E_0 the rest mass of proton (= 938 MeV), T the kinetic energy of proton (= 1 GeV), $(\delta\theta_M)_{ch}$ the maximum angle below which the scattered proton does not hit the wall of the vacuum chamber, and

$$\chi_\gamma = 1.20\,\delta\theta_m\,(1 + 3.33\gamma^2)^{1/2} \quad ,$$

where $\gamma = Z/(137\beta)$, $\beta = v/c$, $\delta\theta_m = \lambda\!\!\!^{-}_0/a$, $\lambda\!\!\!^{-}_0$ is the de Broglie wave length of the incident proton, and a is the radius of the struck atom (= $5.3 \times 10^{-11}\,Z^{-1/3}$). Provided that the foil-hitting probability is 10 % and a carbon foil of 250 mg/cm^2 is used, the maximum emittance growth, that protons injected at the beginning suffer, is 0.23 (πmm·mrad) in the vertical plane. It should be remembered that these values obtained by formula (6) are r.m.s. values. However, this doesn't matter in such the situation where the emittance of the ring beam is as large as 30 πmm·mrad and filled by the phase-space painting.

The relation between the thickness t (μg/cm^2) of a carbon foil and its stripping efficiency for an H° beam is given as follows. The number of atoms in a unit area x (atoms/cm^2) is

$$x = 5.016 \times 10^{16}\,t \quad . \tag{7}$$

Provided that fractions of H° atoms and stripped protons are N° and N$^+$ respectively after the beam passed a thickness x in the carbon foil, then

$$-\frac{dN^\circ}{dx} = \sigma_{01}\,N^\circ \tag{8}$$

$$N^+ = 1 - N^\circ \quad , \tag{9}$$

where σ_{01} is the cross section for H° atoms to be converted to protons. As for σ_{01}, there are many experimental data in the energy region up to a few tens MeV [12] but for higher energies only two data points at 200 MeV and 800 MeV. The data at 800 MeV were taken using a plastic film (Formvar) [13]. Theoretical calculations found in reference [12] shows a good fit to data at low energy. But both data at higher energies are a little smaller than the theoretical values. Therefore, we use a value of σ_{01} a little smaller than the theoretical value for a 1 GeV H° atom, that is

$$\sigma_{01} = 3 \times 10^{-19}\ \mathrm{cm}^2 \quad . \tag{10}$$

Then we can estimate the dependence of N° and N^+ on t by eqs. (7) ~ (10). The result is shown in Fig. 13. As the figure indicates, 250 $\mu g/cm^2$ or more is needed for the foil thickness, in order to make the stripping efficiency no less than 98 %.

4.2 Foil shape, support and its lifetime

Reducing the foil-hitting probability, namely the probability that particles in beam hit the foil, as little as possible is a new subject that is given rise by the experience of the PSR and the requirement of such a high energy and high intensity synchrotron as the I-A ring. One effective way to reduce the foil-hitting probability is to apply properly the technique of phase-space painting to the beam injection. Another effective method is expected if we can use a new type of stripping foil that is shown in Fig. 14. When a small beam is injected at the unsupported corner of the foil and the painting is performed as described in the following section, the probability will be reduced to no more than 10 %.

It is rather easy to mount a carbon foil with a thickness of about 250 $\mu g/cm^2$ on such a support as is shown in Fig. 14. Carbon foils with such a thickness are sufficiently strong against a mechanical shock. We can reform the shape of the unsupported corner with a pair of scissors. One question is whether heating by beam passage deforms the unsupported corner so seriously that a larger part of the injected beam misses the foil. A heating test of the unsupported corner, that we did using an electron beam welder, did not show any serious deformation and suggested that the foil is very promising.

There is very little information on the lifetime of such a carbon foil in bombardment by a high intensity 1 GeV proton beam. As the beam energy is very high, energy dissipation per unit mass of the foil is rather little, but the radiation damage becomes more serious. We know from the literature that the lifetime of 200 $\mu g/cm^2$ carbon foil at the PSR is considerably long. However we don't know anything about the influence of the unusual supporting method of our foil.

4.3 Beam loss due to large angle scattering

When beam particles pass the foil, some particles are scattered to a large angle by the Coulomb scattering or the nuclear scattering. If the Courant-Snyder constant (C-S const.) of the scattered particle becomes larger than the ring acceptance, the particle will be lost at the wall of the vacuum chamber. As $\beta_h = 14.8$ m and $\beta_v = 5.14$ m at the foil, the critical scattering angle θ_c's, at which the C-S const. equals to the ring acceptance (120 πmm·mrad), are

$$\theta_c^h = 2.8 \text{ mrad} \tag{11}$$

$$\theta_c^v = 4.8 \text{ mrad} \tag{12}$$

As the angular distribution of the nuclear scattering expands to all of the polar angle with a gentle slope, almost all particles scattered by the nuclear interaction go beyond the critical angle and are lost. The total cross section of the elastic scattering of a 1 GeV proton by ^{12}C has been measured to be 370 mb [14]. Thus the loss rate due to the nuclear reaction is 4.6×10^{-6} for a single pass through a 250 $\mu g/cm^2$ carbon foil, and the loss rate for the total beam is

$$R_n = 1.4 \times 10^{-4} \quad , \tag{13}$$

provided that the foil-hitting probability is 10 %.

Loss rate R_c due to the Coulomb scattering can be estimated by the formula (13.114) given in J.D. Jacksons' text "Classical electrodynamics" [15].

$$R_c = \pi x \left(\frac{z\,Ze^2}{pv}\right)^2 \cdot \frac{1}{\theta_c^2} \quad . \tag{14}$$

When the 1 GeV proton beam passes a 250 $\mu g/cm^2$ carbon foil, (14) reduces to $R_c = 1.33 \times 10^{-11} \cdot \theta_c^{-2}$. Thus we have for the I-A ring

$$R_c^h = 5.1 \times 10^{-5} \quad , \tag{15}$$

$$R_c^v = 1.7 \times 10^{-5} \quad . \tag{16}$$

Finally, we obtain the total loss rate R_t due to large angle scattering from (13), (15) and (16),

$$R_t = R_n + R_c^h + R_c^v = 2.1 \times 10^{-4} \quad . \qquad (17)$$

4.4 Beam loss due to single Coulomb scattering

As is well known, energy loss of a fast ion in the passage through a foil distributes to far above the mean value. If the energy loss in the stripping foil becomes very large,the proton can not be captured in the RF bucket and will soon be lost. We here try to estimate the loss rate due to large energy loss as the fraction of protons whose energy losses exceed the critical value E_c. Because the energy spread of the injected H^- beam is set as $\pm$ 0.1 % and that of the ring beam as $\pm$ 0.2 %, E_c may be 0.1 % of the beam energy, that is

$$E_c = 1.0\,\text{MeV} \quad . \qquad (18)$$

To estimate the contribution from the multiple scattering, we integrate the Vavilov distribution [16],[17] over the high energy tail. In our case, the Vavilov distribution reduces to the Landau distribution [18], because the parameter κ is very small ($= 2.25 \times 10^{-4}$). κ is the ratio of the mean energy loss over the path length to the largest energy-transfer possible in a single collision with an electron. However we here restrict ourselves to a simple and clear estimation of the loss rate Rs due to a single Coulomb scattering, using the formula [19] of the collision probability for particles of mass m and spin 1/2 which has been calculated by Bhabha

$$\Phi_{col}(E,E')dE' = \frac{2Cm_ec^2}{\beta^2} \cdot \frac{dE'}{(E')^2}\left[1 - \beta^2 \frac{E'}{E'_m} + \frac{1}{2}\left(\frac{E'}{E+mc^2}\right)^2\right] \quad , \qquad (19)$$

where E is the incident energy, E' the energy loss, $C = 0.150\ Z/A$ ($g^{-1}cm^2$), m_e the electron rest mass and E'_m the maximum energy transferable to an electron in a single collision. For a 1 GeV proton

$$E'_m = 3.34\,\text{MeV} \quad . \qquad (20)$$

Provided that the foil-hitting probability is 10 %, the average number of foil passage is 30. When the thickness of the carbon foil is 250 $\mu g/cm^2$, the loss rate R_S is

$$R_S = \int_{E_c}^{E'_m} 30 \times 2.5 \times 10^{-4}\, \Phi_{col}(E,E')dE' = 3.2 \times 10^{-4} \quad . \qquad (21)$$

5. Phase-space painting

There are two purposes with respect to the phase-space painting. One is to make particle distribution over the ring beam cross section as uniform as possible. The other is to make the foil-hitting probability as low as possible. For these purposes, we fix the injection point on the unsupported corner of the stripping foil and vary the bump orbit in both the horizontal and vertical planes.

When the injected beam emittance is very small, an elliptic beam with uniform particle distribution is formed by varying the bump orbit in such a way that the trace of the orbit at the foil location depicts an ellipse centered on the injected beam. Figs 15 and 16 show two cases in which the method is applied to the phase-space painting for the I-A ring beam. The difference between these cases is in the direction of varying the bump orbit for the painting. In the case (1), Fig. 15, the bump orbit is varied from the point (67.6, 8) to (85.3, 0). This variation is realized by the time dependence of the coordinates (x and y) shown in the figure. Then, the beam while being stacked ($0 \leq t \leq T$) moves toward the inside of the foil. Therefore the foil-hitting probability becomes relatively high. Nevertheless, it is at most 15 %. In the case (2), the bump orbit is varied in the inverse direction, as is shown in Fig. 16. Then the beam while being stacked gradually separates from the foil and the foil-hitting probability becomes as low as 8.3 %.

To reduce the foil-hitting probability, it is effective to form a square beam. Fig. 17 shows an example of application to the I-A ring. Then, the foil-hitting probability becomes as low as about 6 %. The time dependence of the coordinate shown in the figure does not give a uniform but an elliptic distribution in each direction if the emittance of the injected beam is very small.

Because the emittance of the injected H^0 beam is not negligibly small, it is expected to be hard to form an ideal beam with uniform distribution only by the method mentioned above. In order to form a beam as uniform as possible, it will be necessary to make the power supply of the bump magnet flexible and to search the best way of the bump orbit variation. Of course, even in these cases, it is also necessary to reduce the foil-hitting probability to no more than 10 %. However, it will be enough possible to realize such a low foil-hitting probability by means of proper phase-space painting and a stripping foil with an unsupported corner.

6. Summary

On designing the injection system of the I-A ring, the Lorentz stripping phenomenon should be carefully coped with.

· The direct H^- injection method is hard to apply, because the straight section is too short to install the beam transport system for the residual H^- beam in the downstream of the stripping foil. (See Appendix III.)

· The H^0 injection method is applicable, when the following conditions are fulfilled as described in the text:

(1) Two special components should be prepared. One is the stripping magnet that has a maximum field no less than 1.8 T and also a field gradient no less than 1.3 T/cm. The other is a stripping foil that has a thickness of about 250 $\mu g/cm^2$ and also an unsupported corner.

(2) The stripping foil should be placed between a QF magnet and the B magnet in the upstream of it, and should be positioned outside the ring acceptance in the horizontal plane.

(3) The stripping magnet should be placed as near as possible to the foil, upstream of the B magnet.

(4) The H^0 beam should be formed not only to fit the emittance ellipse of the ring beam but also to be as small as possible on the foil and injected into the unsupported corner of the foil.

(5) The bump orbit should be formed in the ring both in the horizontal and vertical plane, and varied not only to paint the H^0 beam over the emittance ellipse of the ring beam but also to reduce the foil-hitting probability to no more than 10 %.

(6) An acceptance of 120 πmm·mrad should be guaranteed around the bump orbit at the end of injection.

Acknowledgement

The authors are very grateful to Professors M. Kihara and Y. Kamiya for stimulating discussions and their encouragement given throughout this work. They also wish to express their heartfelt thanks to Dr. Robert A. Jameson of the Los Alamos National Laboratory, USA for reading the draft, giving many useful comments and kindly acting as a middleman of early debate on this subject between people of the Los Alamos PSR and the authors.

References

[1] " Report of the design study on the compressor / stretcher ring of the Japan Hadron Project [I] " ; JHP-11, KEK Internal 88-9, Sept. 1988

[2] G.M. Stinson et al., Nucl. Instr. and Meth. 74, 333 (1969).

[3] L.R. Scherk, Can. J. Phys., 57, 558 (1979).
[4] D.W. Hudgings, IEEE Trans. Nucl. Sci. Vol.NS-26, No.3, 3556 (1979).
[5] A.J. Jason et al., IEEE Trans. Nucl. Sci. Vol.NS-28, No.3, 2704 (1981).
[6] G.P. Larence et al., IEEE Trans. Nucl. Sci. Vol.NS-32, No.5, 1985, pp.2662-2665.
[7] G.P. Lawrence, Proc. 1987 IEEE Part. Acc. Conf., March, 1987, pp.825-829.
[8] R.J. Macek et al., Proc. 1st Eur. Part. Acc. Conf., June, 1988.
[9] The field distribution is calculated by Mr. Noriyuki Matsumoto of Tokin Corporation.
[10] H.H. Andersen and J.F. Ziegler, "Hydrogen Stopping Powers and Ranges in All Elements" (Pregnum Press, New York, 1977).
[11] R.K. Cooper and G.P. Lawrence, IEEE Trans Nucl. Sci. Vol.NS-22, No.3, 1916 (1975).
[12] R.C. Webber and C. Hojvat, IEEE Trans. Nucl. Sci., Vol.NS-26, No.3, June 1979, pp.4012-4014.
[13] O.B. van Dick et al., AIP Conf. Proc. No.69, "Polarization Phenomena in Nuclear Physics", 1980, pp.985-987.
[14] H. Palevsky et al., Phys. Rev. Letts. 18 (1967) 1200.
[15] J.D. Jackson, "Classical Electrodynamics", John Wiley and Sons, Inc., New York, 1962.
[16] P.V. Vavilov, Zh. Exper. Teor. Fiz. 32, 320 (1957) Transl., JETR, 5, 749 (1957).
[17] S.M. Seltzer and M.J. Berger, Nucl. Sci. Series No.39, National Research Council, pp.187-203.
[18] L. Landau, J. Exp. Phys. (USSR), 8, 204 (1944).
[19] B. Rossi, "High Energy Particles", Prentice-Hall Inc., Englewood Cliffs, N.J. 1952.

Appendix I Outline of the I-A Ring

The I-A ring is a compressor / stretcher ring that reforms the 1 GeV H^- beams from a linac to proton beams with various time structures and supplies them to the Neutron and Meson Arenas. The 1 GeV H^- beam is supplied as the beam pulse of 400 μsec long at a repetition rate of 50 Hz. Each pulse has a pulse-train structure with pulses about 200 nsec long and separated by about 130 nsec. These H^- beam pulses are converted to proton beam pulses at the injection point of the I-A ring. Proton beam pulses captured in the ring are accumulated to form two beam bunches of about 200 nsec.

One of these bunches is ejected just after the injection for the Neutron Arena. Then the other bunch is reformed in the ring to various bunch lengths in response to users requirements and supplied to the Meson Arena. In the compressor mode the beam bunch is compressed, at the nimimum, to such an extremely short bunch as about 20 nsec long. On the other hand, the beam is ejected as a continuous beam lasting for about 15 msec by the slow extraction method in the stretcher mode.

The plan view of the I-A ring is shown in Fig. 1. It has 16 FODO cells and optical parameters of a single cell is shown in Fig. 2. Main parameters of the I-A ring and the 1 GeV H^- beam are listed in Table 1 and 2 respectively.

Appendix II Lorentz Stripping

As the second electron of the H^- ion is weakly bound with a low binding-energy of 0.755 eV, it can be detached by a strong electric field and the H^- ion is converted to the H° atom. This stripping phenomenon also occurs in the action of the Lorentz force, because the Lorentz force is equivalent to the electric field. When an H^- ion with a velocity βc traverses in a magnetic field B, the equivalent electric-field in the rest frame of the H^- ion is given

$$E = \gamma\beta c\, B \quad . \tag{A-1}$$

Then the rest-frame life time τ of the H^- ion is expressed as

$$\tau = (A_1/E) \exp (A_2/E) \quad , \tag{A-2}$$

where A_1 and A_2 are constants which are determined to fit the experimental results. For A_1 and A_2 two different sets of values are found in literatures by G.M. Stinson et al. [2], and by A.J. Jason [5]. The former gives $A_1 = 7.96 \times 10^{-6}$ V·s/m and $A_2 = 4.256 \times 10^9$ V/m, and the latter $A_1 = 2.47 \times 10^{-6}$ V·s/m and $A_2 = 4.49 \times 10^9$ V/m. In this report we used the latter set of values.

How serious the Lorentz stripping is can be seen in Fig. 18, where are shown B dependences of flight-path length in which the H^- fraction in the 1 GeV H^- beam reduces to 0.999, 1/e and 0.001. When we want to avoid a beam loss of 0.1 %, the allowable length of the magnetic field is 50 cm for B = 0.425 T and 7 cm for B = 0.45 T. On the other hand, more than 99.9 % of the H^- beam can be stripped in 1 mm in a magnetic field of 1.8 T.

Variation of the H^- fraction alo ζ the beam path is given by

$$df = -\frac{f}{\gamma\beta c\tau} \cdot ds \quad , \tag{A-3}$$

where f is the H^- fraction in the beam and s is the length along the beam path. If B is given as a function of s ; B = B(s), then we can derive the fraction along the beam path as

$$f(s) = \exp\left[-\int_0^s \frac{B(s)}{A_1} \exp\left(\frac{-A_2}{\gamma\beta c B(s)}\right) ds\right] \quad . \tag{A-4}$$

Appendix III Direct H^- Injection into the I-A Ring

At first we tried to apply the direct H^- injection to the I-A ring. We soon found that it was very difficult to guide the residual H^- beam remaining downstream of the foil to a beam dump. If all of the injected H^- beam passed through a stripping foil of sufficient thickness, the residual H^- beam clearly would be negligible. But in the case of the I-A ring, where the foil-hitting probability should be reduced to as low as 10 %, the H^- beam must be injected just inside the foil edge. In this situation, we must expect that part of the H^- beam halo or the beam edge will miss the foil even if the operation condition is carefully adjusted. Although the amount of such a part is probably very little, it may produce a serious problem because a loss of 0.1 % of the beam will make the same residual activity as at the extraction section of the KEK-PS. Therefore an additional beam transport system is needed to guide the part of the H^- beam missing the foil to a beam dump.

Fig. 19 shows the case in which the stripping foil is set in the midway of a long straight section. To form a bump orbit that passes the stripping foil, two types of bump orbit must be superposed. One is formed using the focusing forces of the lattice and the other using a set of four bump magnets in the straight section. Further two septum magnets are needed, to make both the injected and residual H^- beam clear the neighbouring Q magnets. The field of these septum magnets should be as low as 0.4 T to avoid the Lorentz stripping. Then after we secure the length of the injection septum magnet, the space left is too short for the other septum to make the residual H^- beam clear the neighbouring Q magnet. So the residual H^- beam will be lost in the straight section.

Fig. 20 shows another case, in which the bump orbit is formed with the Q_F magnet placed upstream of the B magnet and other three bump magnets. The stripping foil is set in front of the Q_F magnet and at a displacement of 80 mm from the central orbit. The bump orbit, that penetrates the foil, also passes the Q_F magnet at a distance of 92 mm from the central orbit. This orbit is the outermost bump orbit that is guaranteed

the acceptance of 120 πmm·mrad. The deflection angle of this orbit in the QF magnet is 22 mrad. Therefore, when the H^- beam is directly injected to the stripping foil along the bump orbit, the residual H^- beam is deflected outside by 22 mrad and injected into the B magnet at the displacement of 125.5 mm from the central orbit. As the magnetic field is 0.8 T, the H^- beam will soon be converted to H^0 by the Lorentz stripping and lost around the B magnet. In such an arrangement, it is very hard to make the residual H^- beam clear not only the main field but also the fringing field of the B magnet.

Figure Captions

Fig. 1 Plan view of the JHF I-A ring. Main parameters of the I-A ring are listed in Table 1.

Fig. 2 Betatron functions and dispersion function for a single cell. Parameters of the magnets are shown in Table 1.

Fig. 3 The H^0 injection scheme for the I-A ring. The closed orbit in the ring is properly distorted during injection to conduct the formed proton beam into the ring orbit.

Fig. 4 The process to search parameters of the beam whose size at the foil is the minimum on the condition that it forms a waist at the center of the stripping magnet. The emittance ellipse of the resultant beam is shown in the right top.

Fig. 5 The process to search parameters of the beam fitting to the ring beam emittance ellipse in the vertical plane where the beam angle is enlarged by the stripping magnet.

Fig. 6 Injection of the H^0 beam into the ring beam emittance ellipse. $\Delta\psi_x$ and $\Delta\psi_y$ are necessary phase advances of betatron oscillation between the upstream bump magnet and the foil for the H^0 beam to be injected into the indicated position of the ring beam emittance ellipse.

Fig. 7 Relation between the betatron oscillation phase advance from the upstream bump magnet to the foil and the relative position of the H^0 beam to the ring beam in the phase space.

Fig. 8 The injection bump orbit in the horizontal plane. The bump magnet HB1 is placed at a point where the betatron phase precedes the foil by $\Delta\psi_x$. The bump magnet HB2 is also place at π of the betatron phase from HB1.

Fig. 9 The injection bump orbit in the vertical plane. The bump magnet VB1 is placed at a point where the betatron phase precedes the foil by $\Delta\psi_y$. The bump magnet VB2 is placed at π of the betatron phase from VB1.

Fig. 10 The whole arrangement of the H° injection system of the I-A ring. Bump magnets B3's and B4's are installed to form the same injection bump orbit when the tune of the ring is varied.

Fig. 11 Calculated angular distributions of the H° beam downstream of the stripping magnet. Calculation is done using model field distributions shown in the inset.

Fig. 12 The stripping magnet. (a) is the pole shape of the stripping magnet. (b) is an example of the calculated field distribution.

Fig. 13 Calculated thickness dependence of the charge state fraction, when 1 GeV H° beam is injected to a carbon foil. σ_{01} is the cross section of the charge exchange reaction that is used in the calculation.

Fig. 14 The stripping carbon foil with an unsupported corner. (a) its shape and (b) a photograph.

Fig. 15 Painting method (1) to form an elliptic beam.

Fig. 16 Painting method (2) to form an elliptic beam. In this case the resulting foil-hitting probability is lower than in the painting method (1).

Fig. 17 Painting method to form a square beam. In this case the foil-hitting probability is the lowest in the mentioned three methods.

Fig. 18 Calculated flight path of the 1 GeV H^- ion in the magnetic field.

Fig. 19 A trial to apply the direct H^- injection method to the I-A ring. In this case, it is difficult to install a septum magnet that makes the residual H^- beam in the downstream of the foil clear the next quadrupole-magnet.

Fig. 20 A trial to apply the direct H^- injection method to the I-A ring. In this case, the residual H^- beam in the downstream of the foil cannot avoid to be stripped in the main or fringe field of the ring bending magnet and the resultant H° beam will be scattered in the vacuum chamber.

Table 1 Main parameters of the I-A ring

Energy	GeV	1.0
Circulating current (I_{av})	A	6 (max. 12)
Revolution frequency ($f_{rev.}$)	MHz	1.5
Harmonic number (h)		2
RF frequency (f_{RF})	MHz	3.0
Circumference (C)	m	174.88
Average radius (R)	m	27.83
Repetition rate	Hz	50
Average current	μA	200 (400)
Lattice type		FODB
Cell number		16
Long straight section	m	5.653
Horizontal tune (ν_x)		4.25
Vertical tune (ν_y)		3.25
Bending magnet		
Bending angle	deg.	22.5
Magnetic field	T	0.8
Length	m	2.777
Bending radius	m	7.072
Magnetic gap	mm	132
Quadrupole magnet		
strength $(B'l/B\rho)_F$	1/m	0.2447
strength $(B'l/B\rho)_D$	1/m	-0.2315
Length	m	0.5
Bore radius	mm	116
Beam		
Emittance (ε_x)	π·mm·mrad	30
Emittance (ε_y)	π·mm·mrad	30
Acceptance (A_x)	π·mm·mrad	120
Acceptance (A_y)	π·mm·mrad	120
Energy spread	%	~±0.2
Max. momentum spread	%	~1.0
Max. momentum acceptance	%	~1.5
Pulse length (at injection)	ns	~200

Table 2 Main parameters of the 1 GeV H^- beam

Energy	GeV	1.0
Repetition rate	Hz	50
Pulse length of beam	μs	400
Duty factor	%	3
Peak current	mA	10 (20)
Average current	μA	200 (400)
Emittance (ε)	π·mm·mrad	1.44(100%)
Energy spread	%	±0.1

Table 3 Summary on the H^- beam and the H^0 beam

Stripping magnet

Location	m	3.812 (upstream of foil)
Gap direction		Horizontal
Gap height	mm	≥11

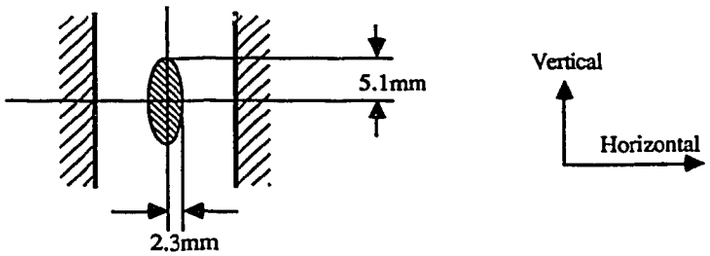

H^- beam at the center of the stripping magnet

		Horizontal	Vertical
β	m	3.674	17.798
α		0	2.325
γ	1/m	0.272	0.360
ε	π·mm·mrad	1.44	1.44
Half width	mm	2.30	5.06
Half angle	mrad	0.63 (waist)	-0.72 (converging)

H^0 beam on the foil

		Horizontal	Vertical
Half width	mm	3.31	4.45
Half angle	mrad	0.63	1.22

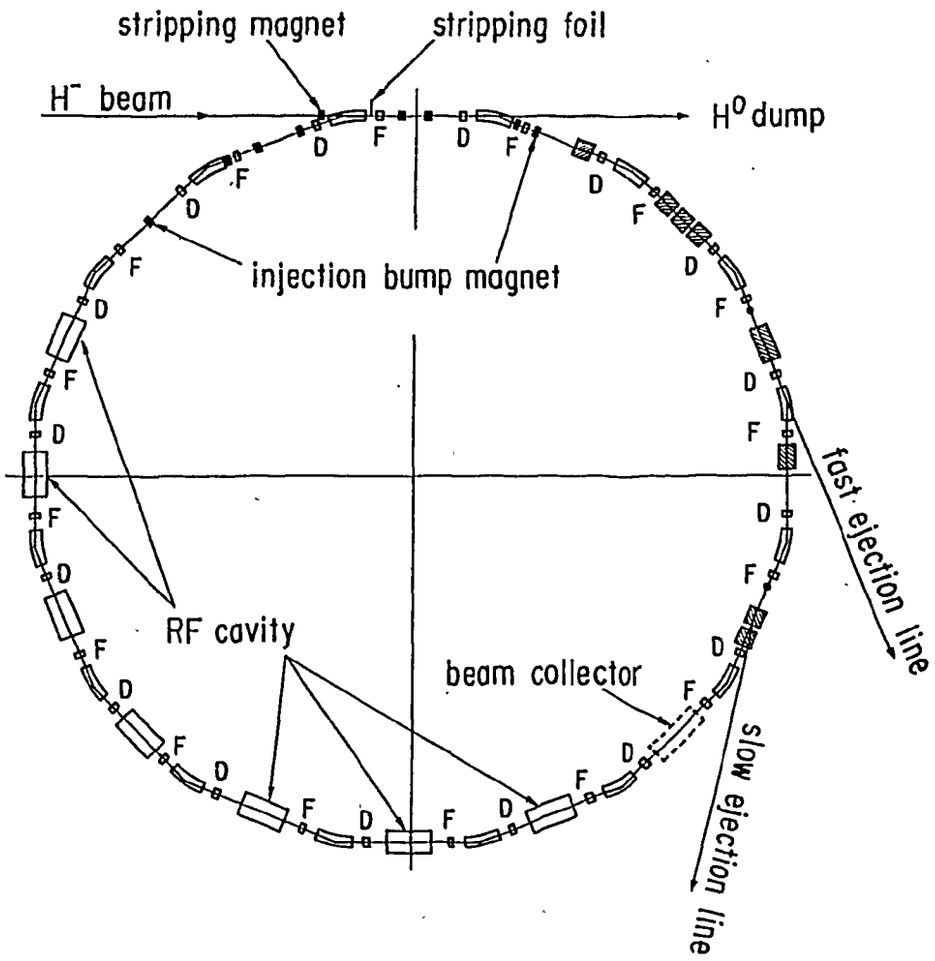

Plan view of the JHF I-A ring

Fig. 1

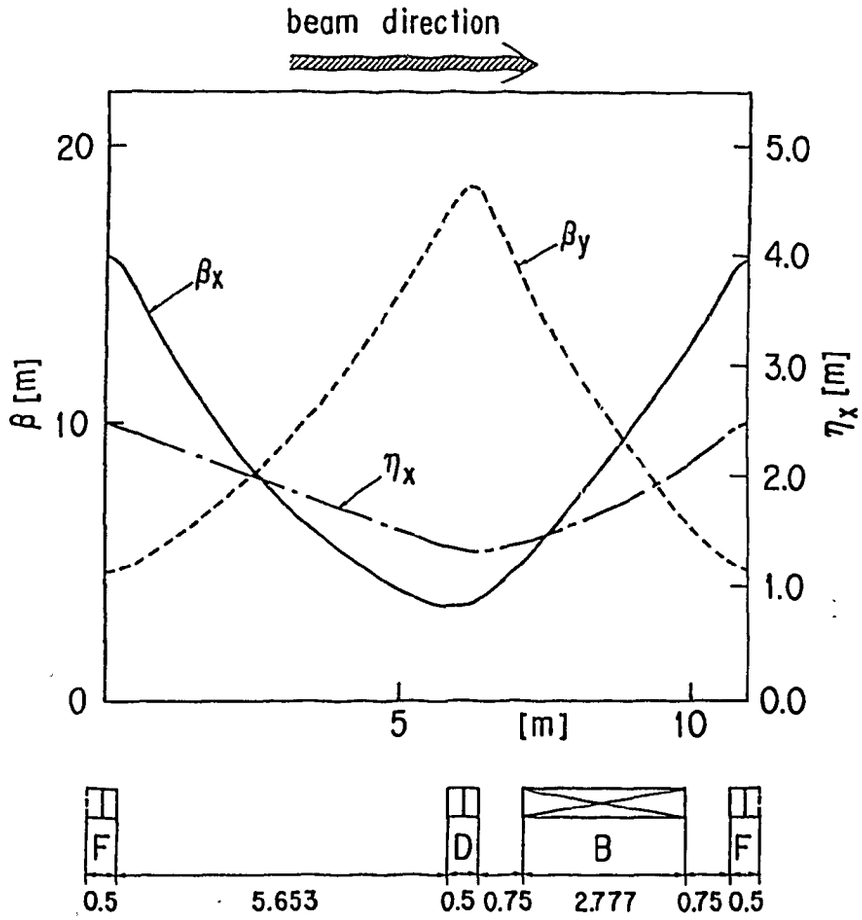

Betatron functions and dispersion function for a single cell

Fig. 2

Fig. 3 H^0 injection scheme for I – A ring

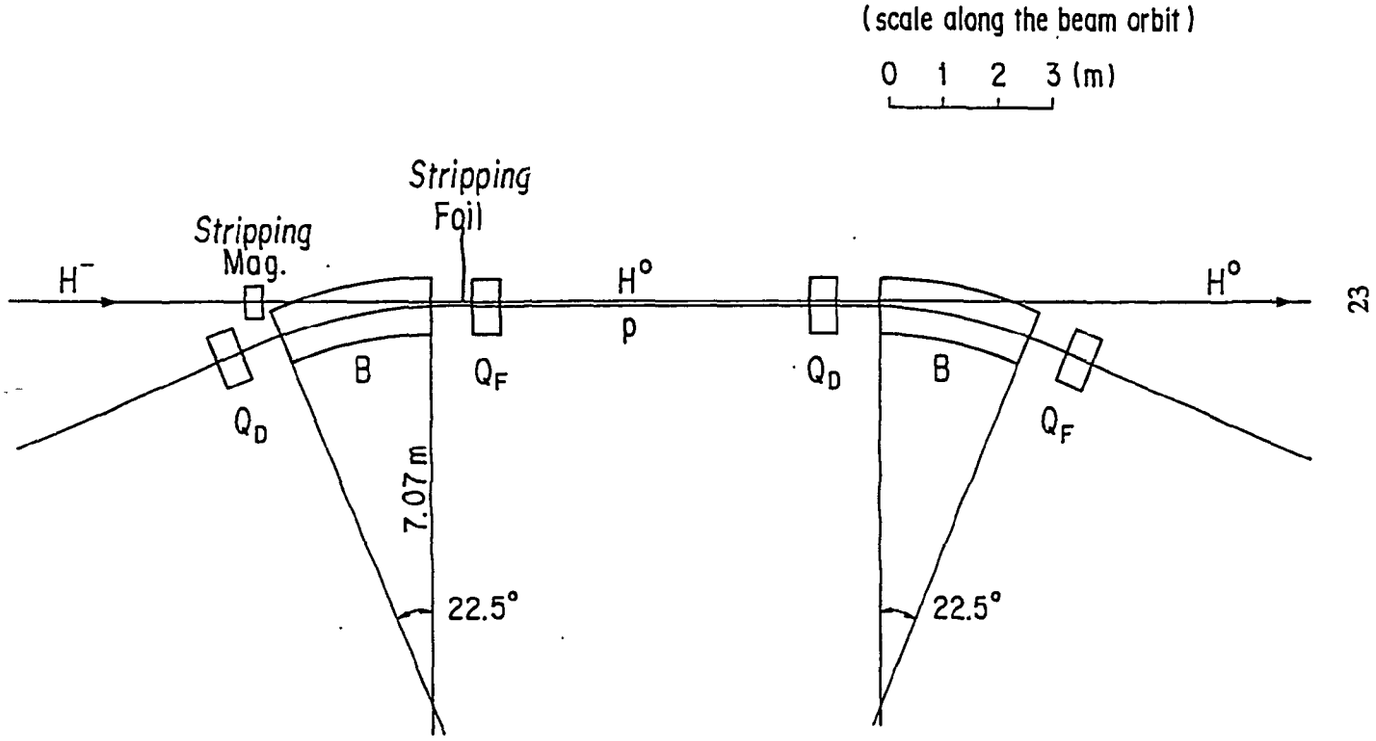

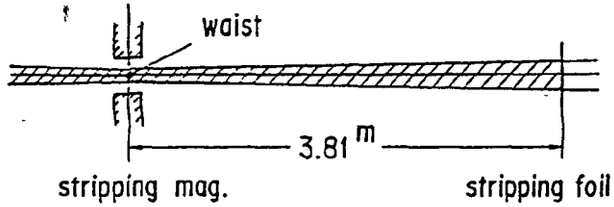

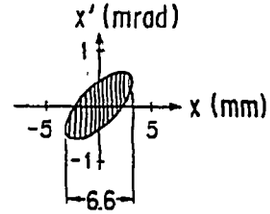

beam emittance : $\varepsilon_h = 1.44$ (πmm·mrad)

H^0 beam on the foil

at the stripping magnet				on the stripping foil		
a	θ	β_s	γ_s	β_f	α_f	γ_f
mm	mrad	m	m^{-1}	m		m^{-1}
1.0	1.44	0.694	1.440	21.619	-5.489	1.440
1.5	0.96	1.563	0.640	10.863	-2.440	0.640
2.0	0.72	2.778	0.360	8.009	-1.372	0.360
2.3	0.626	3.674	0.272	7.626	-1.037	0.272
2.5	0.576	4.340	0.230	7.682	-0.877	0.230
3.0	0.480	6.250	0.160	8.575	-0.610	0.160
3.4	0.411	8.507	0.118	10.222	-0.450	0.118
4.0	0.360	11.111	0.090	12.419	-0.343	0.090

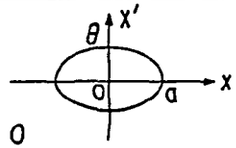

$\alpha_s = 0$

$\beta_f = \beta_s + \gamma_s \ell^2$

$\alpha_f = -\gamma_s \ell$

$\gamma_f = \gamma_s$

$\ell = 3.812$ (m)

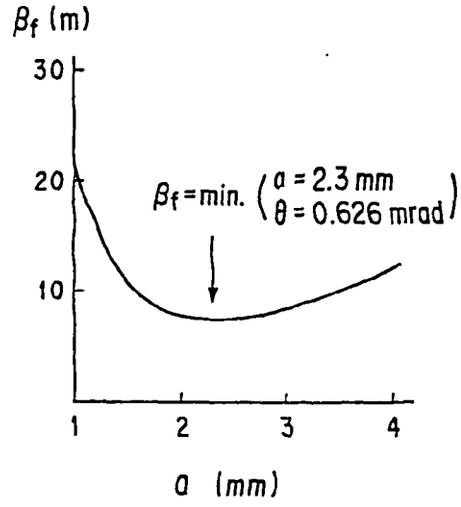

Fig. 4 Beam formation in the gap direction of the stripping magnet

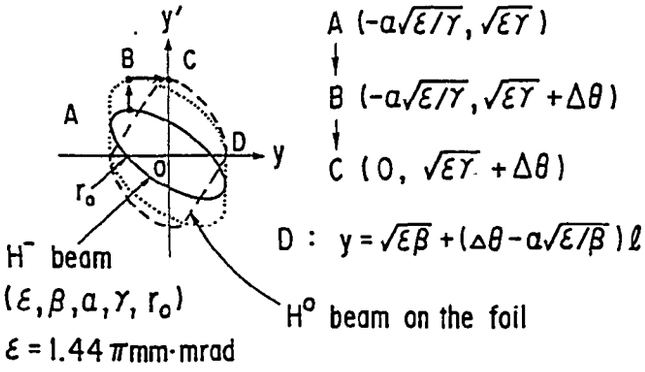

A $(-\alpha\sqrt{\varepsilon/\gamma}, \sqrt{\varepsilon\gamma})$

↓

B $(-\alpha\sqrt{\varepsilon/\gamma}, \sqrt{\varepsilon\gamma} + \Delta\theta)$

↓

C $(0, \sqrt{\varepsilon\gamma} + \Delta\theta)$

D : $y = \sqrt{\varepsilon\beta} + (\Delta\theta - \alpha\sqrt{\varepsilon/\beta})\ell$

$\ell = 3.812$ (m), $\Delta\theta = 0.5$ (mrad)

Condition for C to come on y'-axis :

$$(\sqrt{\varepsilon\gamma} + \Delta\theta)\ell = \alpha\sqrt{\varepsilon/\gamma}. \quad \text{------①}$$

From $r_o = \sqrt{\varepsilon/\gamma}$,

$$\gamma = \varepsilon/r_o^2. \quad \text{-------②}$$

From ①, $\alpha = \ell(\varepsilon/r_o + \Delta\theta)/r_o$. ------③

Further $\beta = (1+\alpha^2)/\gamma$. ----------④

at the stripping mag.				on the foil	
r_o	γ	α	β	$\frac{x'}{\sqrt{\varepsilon\gamma}+\Delta\theta}$	$\frac{x}{\sqrt{\varepsilon\beta}+(\Delta\theta-\alpha\sqrt{\varepsilon/\beta})\ell}$
mm	m^{-1}		m	mrad	mm
1.0	1.440	7.395	38.67	1.94	3.93
1.5	0.640	3.710	23.07	1.46	4.14
2.0	0.360	2.325	17.80	1.22	4.45
2.5	0.230	1.641	16.05	1.08	4.84
3.0	0.160	1.245	15.94	0.98	5.27
3.5	0.118	0.993	16.83	0.91	5.72
4.0	0.090	0.820	18.58	0.86	6.21

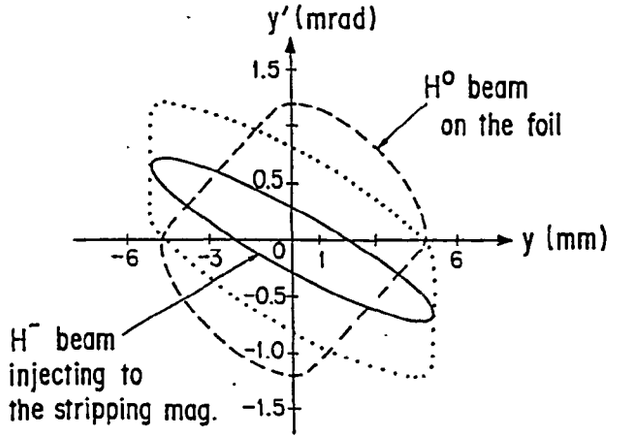

Fig. 5 Beam formation in the vertical plane

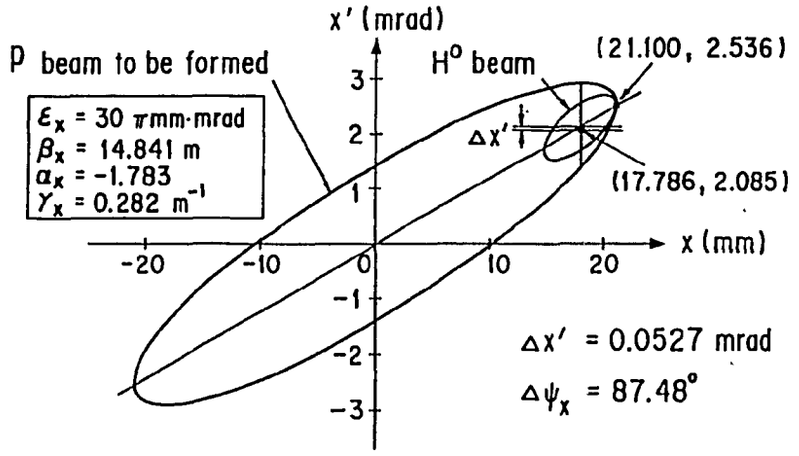

(a) Horizontal plane

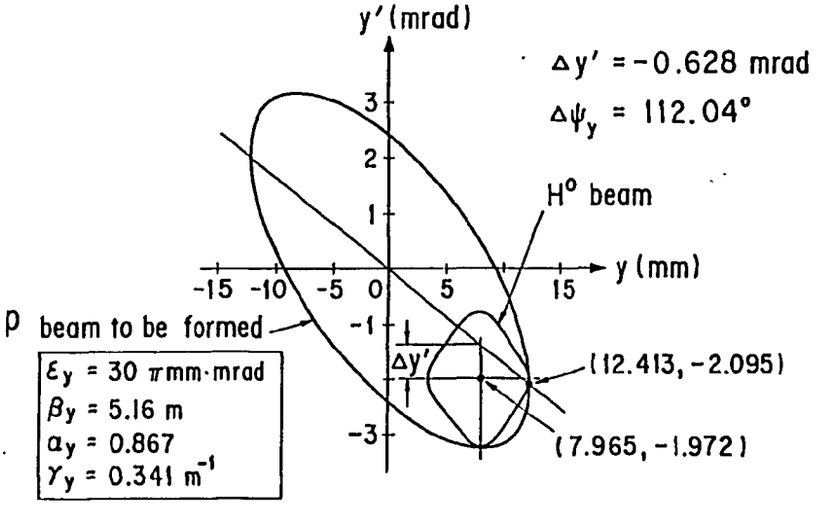

(b) Vertical plane

H° beam injection into the emittance ellipse of the ring beam

Fig. 6

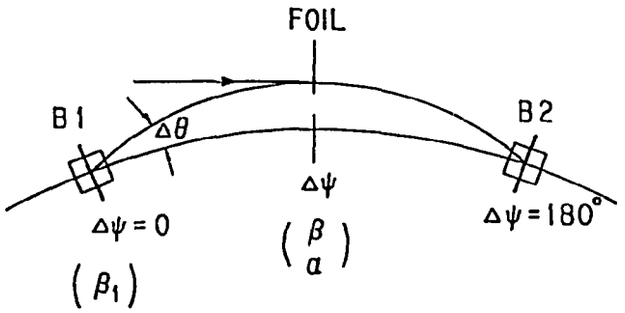

(a) bump orbit

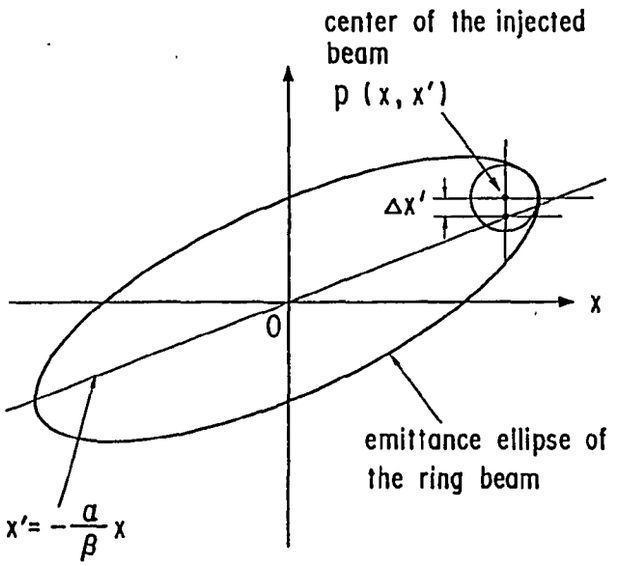

(b) relation between the injected beam and the ring beam in the phase space

Positioning of the bump magnet B 1

Fig. 7

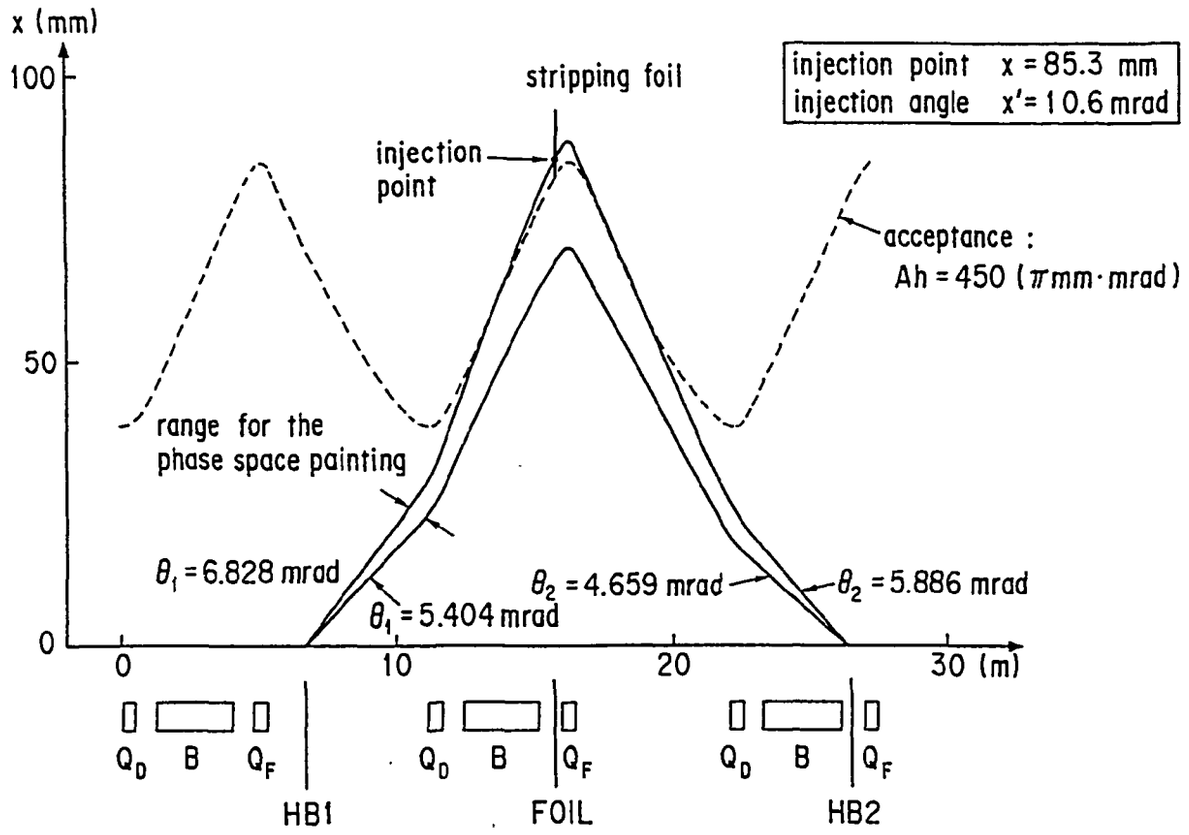

Fig. 8 Injection bump orbit in the horizontal plane

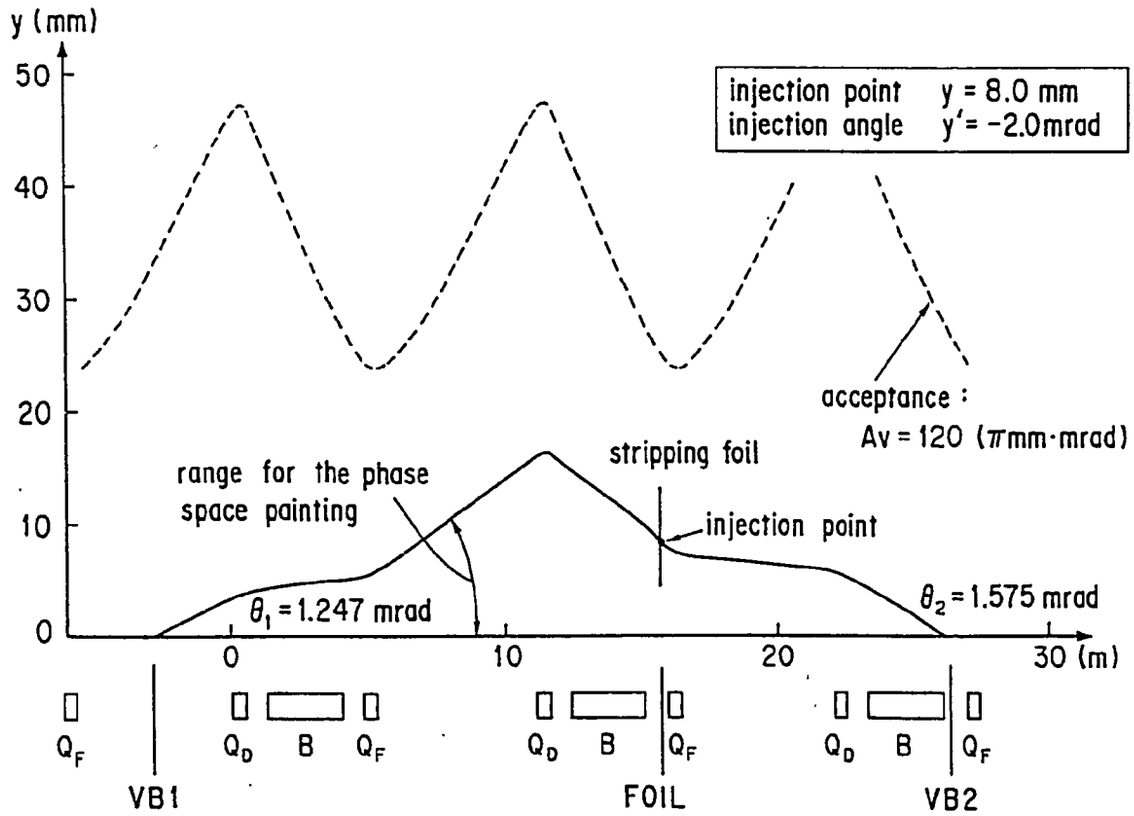

Fig. 9 Injection bump orbit in the vertical plane

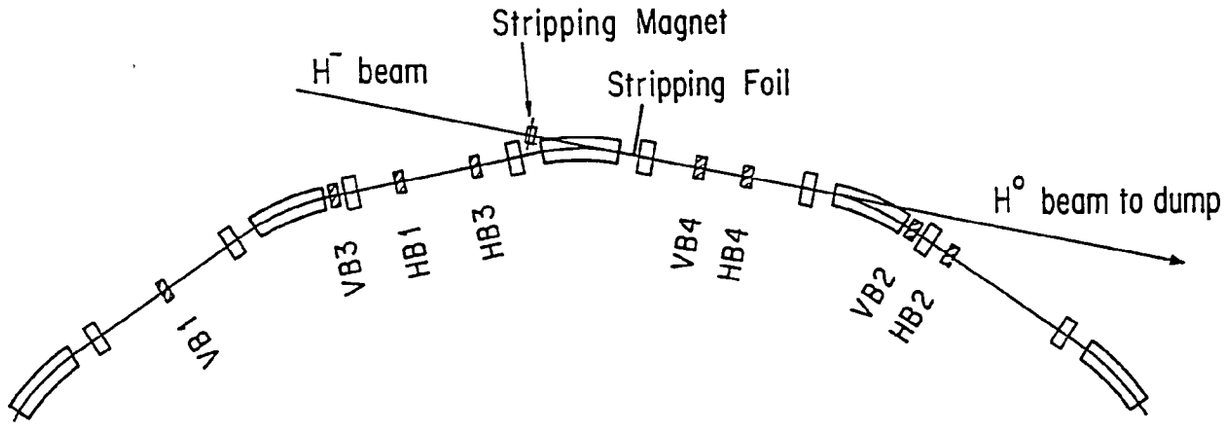

Fig. 10 H° injection system of I-A ring

Fig. 11

Spreading of beam angle by the stripping magnet

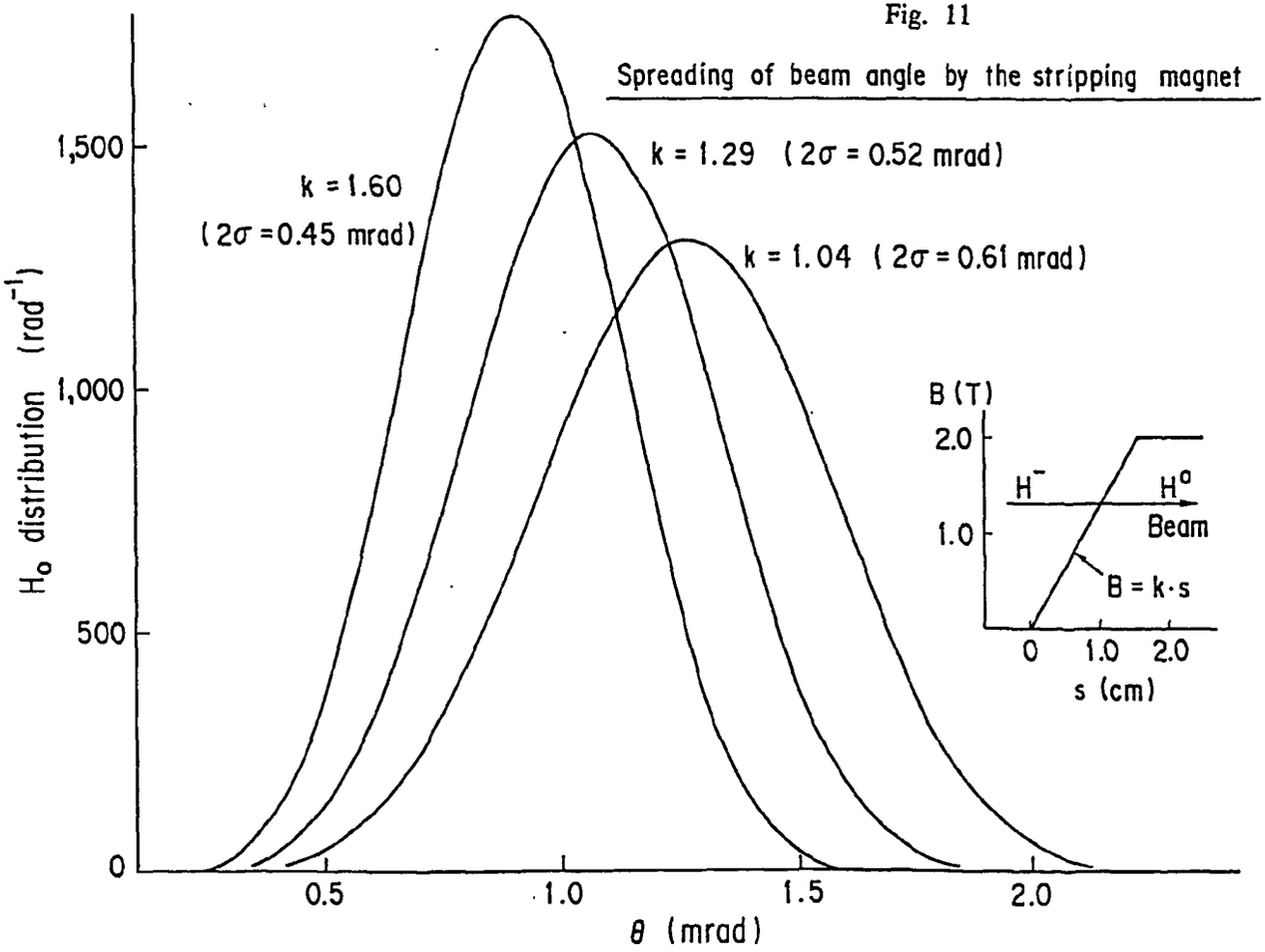

Fig. 12

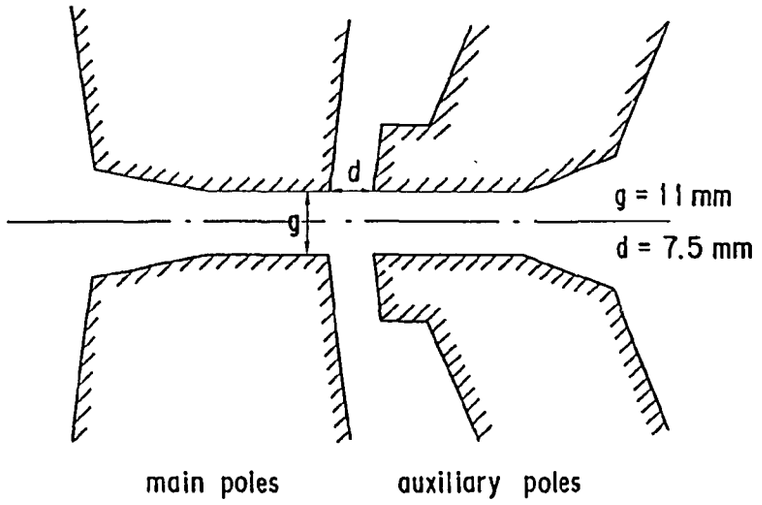

(a) pole shape of the stripping magnet

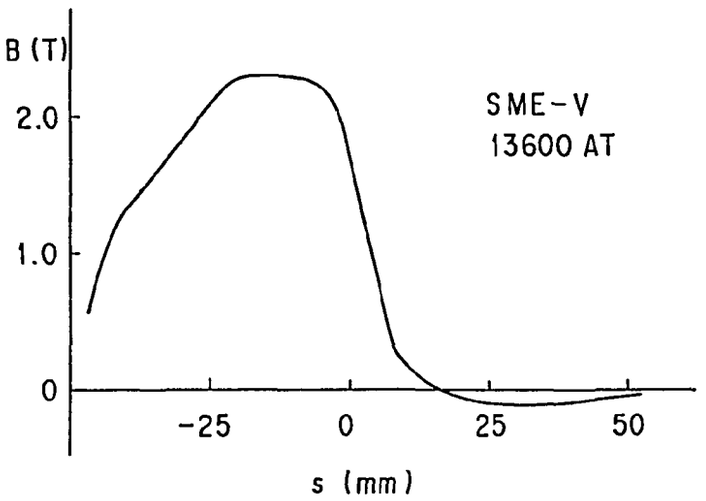

(b) field distribution [9]

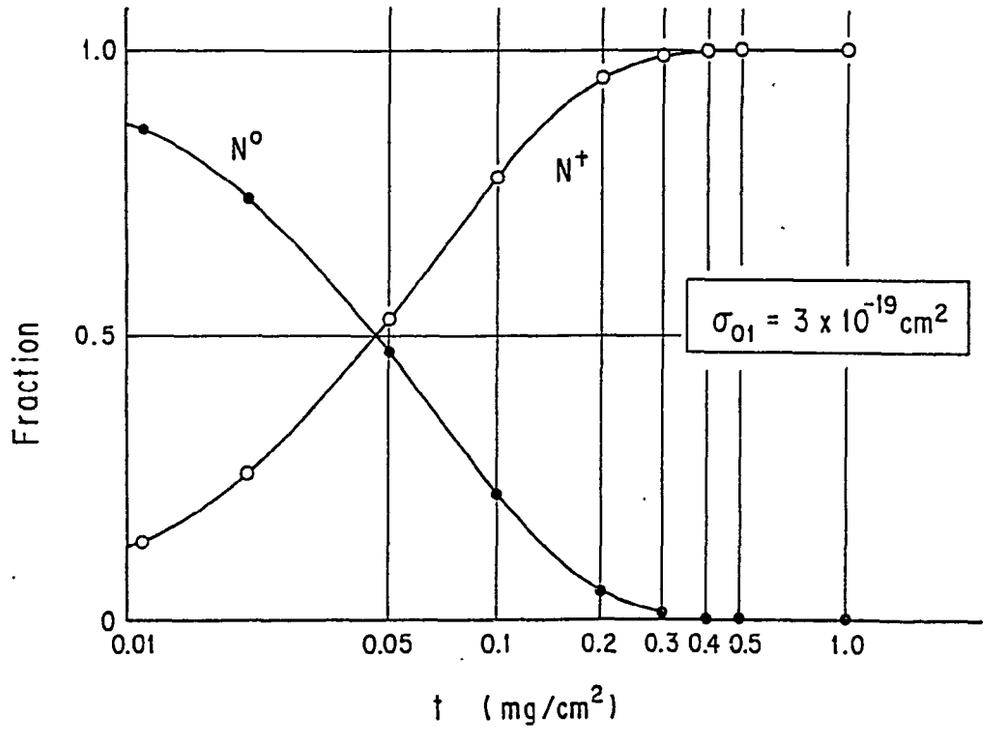

Fig. 13 Thickness dependence of the charge-state fraction, when injecting 1 GeV neutral Hydrogen atom to a carbon foil

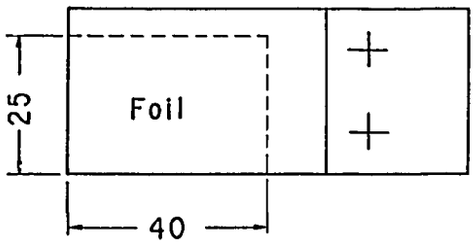

(a) carbon foil and its frame

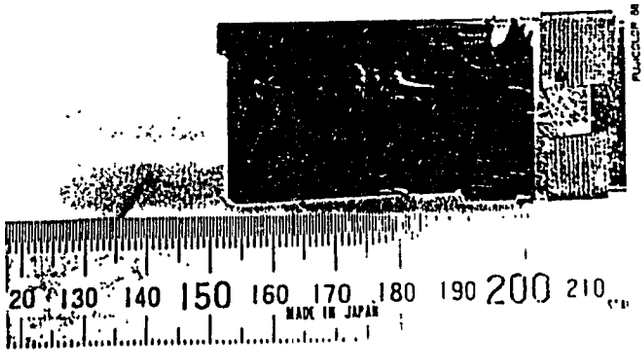

(b) photograph of the stripping foil

Fig. 4

injection point	injection angle
x = 85.3 mm y = 8.0	x′ = 10.6 mrad y′ = −2.0

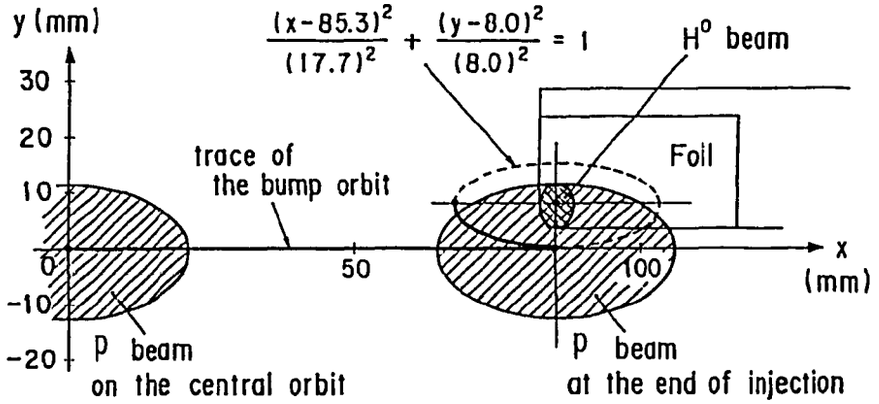

- variation of bump orbit at the foil location

$$x = 85.3 - 17.7\sqrt{1-(t/T)} \quad (\text{mm}) \quad (0 \le t \le T)$$

$$85.3\,(t-te)/(T-te) \quad (\text{mm}) \quad (T \le t \le te)$$

$$y = 8.0 - 8.0\sqrt{(t/T)} \quad (\text{mm}) \quad (0 \le t \le T)$$

- foil hitting probability = 15 %

Formation of an elliptic beam (1)

Fig. 15

injection point	injection angle
x = 85.3 mm y = 8.0	x′ = 10.6 mrad y′ = −2.0

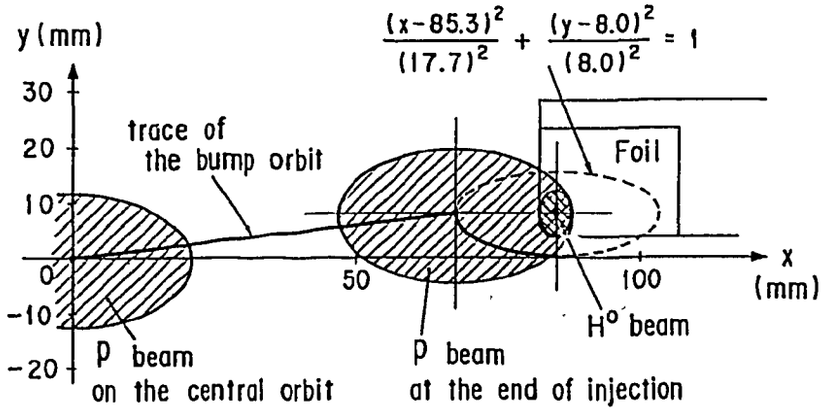

- variation of bump orbit at the foil location

$$x = 85.3 - 17.7\sqrt{(t/T)} \quad \text{(mm)} \quad (0 \le t \le T)$$

$$67.6\ (t-te)/(T-te) \quad \text{(mm)} \quad (T \le t \le te)$$

$$y = 8.0 - 8.0\sqrt{1-(t/T)} \quad \text{(mm)} \quad (0 \le t \le T)$$

$$8.0\ (t-te)/(T-te) \quad \text{(mm)} \quad (T \le t \le te)$$

- foil hitting probability = 8.3 %

Formation of an elliptic beam (2)

Fig. 16

injection point	injection angle
x = 85.3 mm y = 8.0	x' = 10.6mrad y' = -2.0

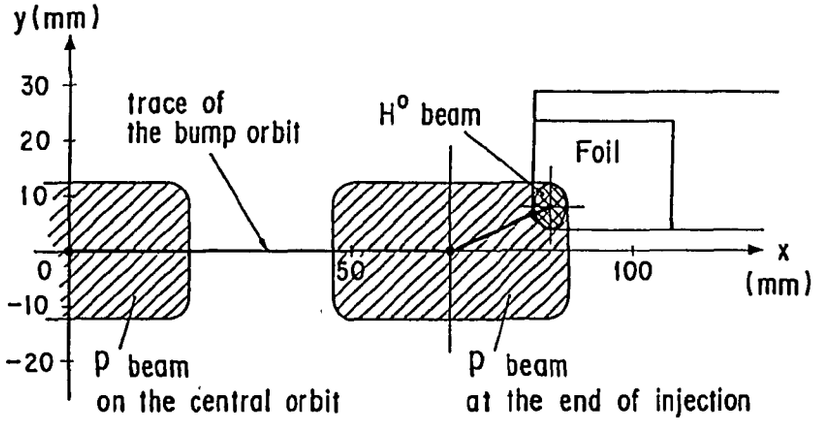

- variation of bump orbit at the foil location

$$x = 85.3 - 17.7\sqrt{(t/T)} \quad (mm) \quad (0 \le t \le T)$$

$$67.6\ (t-te)/(T-te) \quad (mm) \quad (T \le t \le te)$$

$$y = 8.0 - 8.0\sqrt{(t/T)} \quad (mm) \quad (0 \le t \le T)$$

- foil hitting probability = 6 %

Formation of a square beam

Fig. 17

Fig. 18

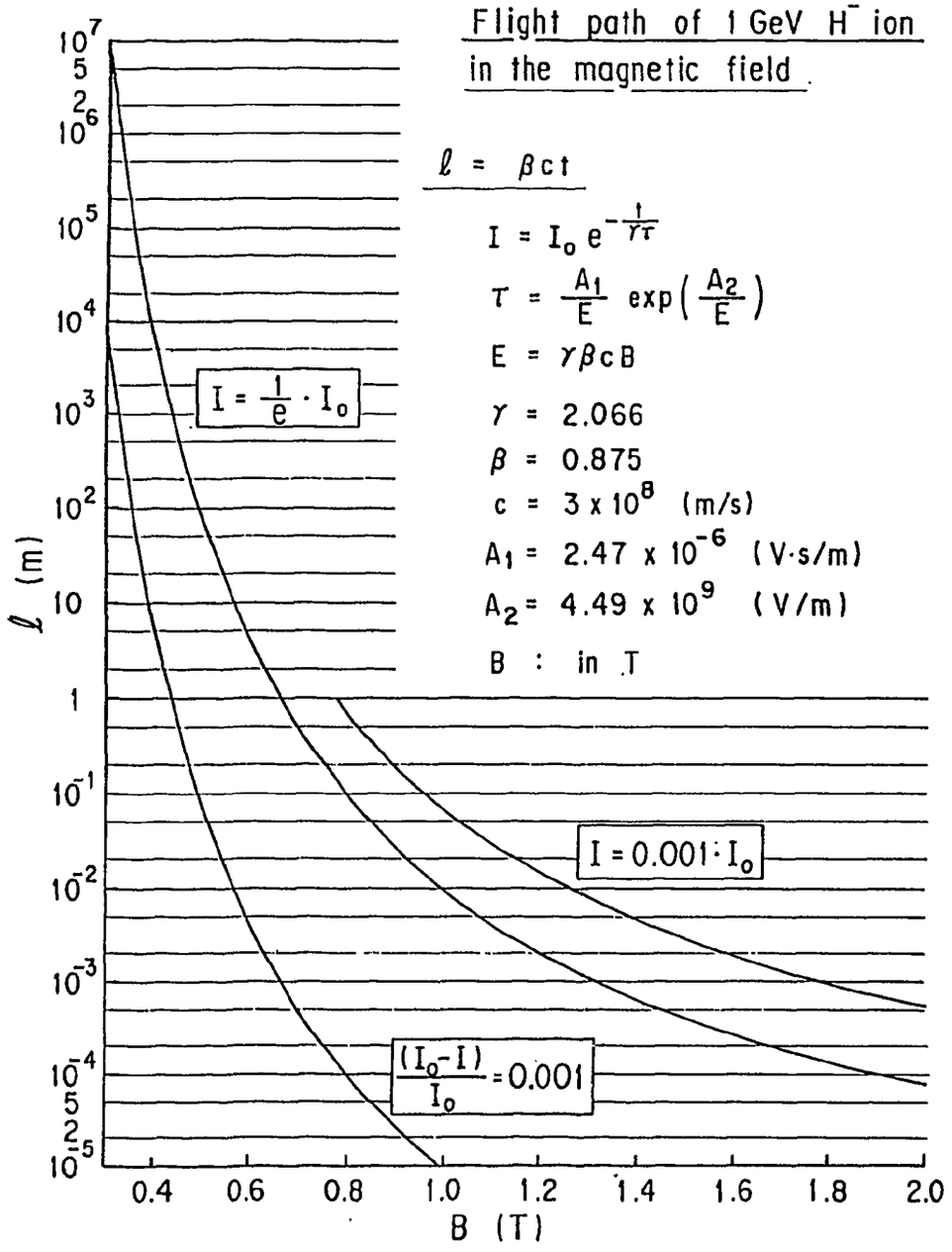
Flight path of 1 GeV H⁻ ion in the magnetic field
ℓ = βct
I = I₀ e^(-1/γτ)
τ = (A₁/E) exp(A₂/E)
E = γβcB
γ = 2.066
β = 0.875
c = 3 x 10⁸ (m/s)
A₁ = 2.47 x 10⁻⁶ (V·s/m)
A₂ = 4.49 x 10⁹ (V/m)
B : in T
I = (1/e)·I₀
I = 0.001·I₀
(I₀-I)/I₀ = 0.001
ℓ (m)
B (T)
10⁷
5
2
10⁶
10⁵
10⁴
10³
10²
10
1
10⁻¹
10⁻²
10⁻³
10⁻⁴
5
2
10⁻⁵
0.4
0.6
0.8
1.0
1.2
1.4
1.6
1.8
2.0

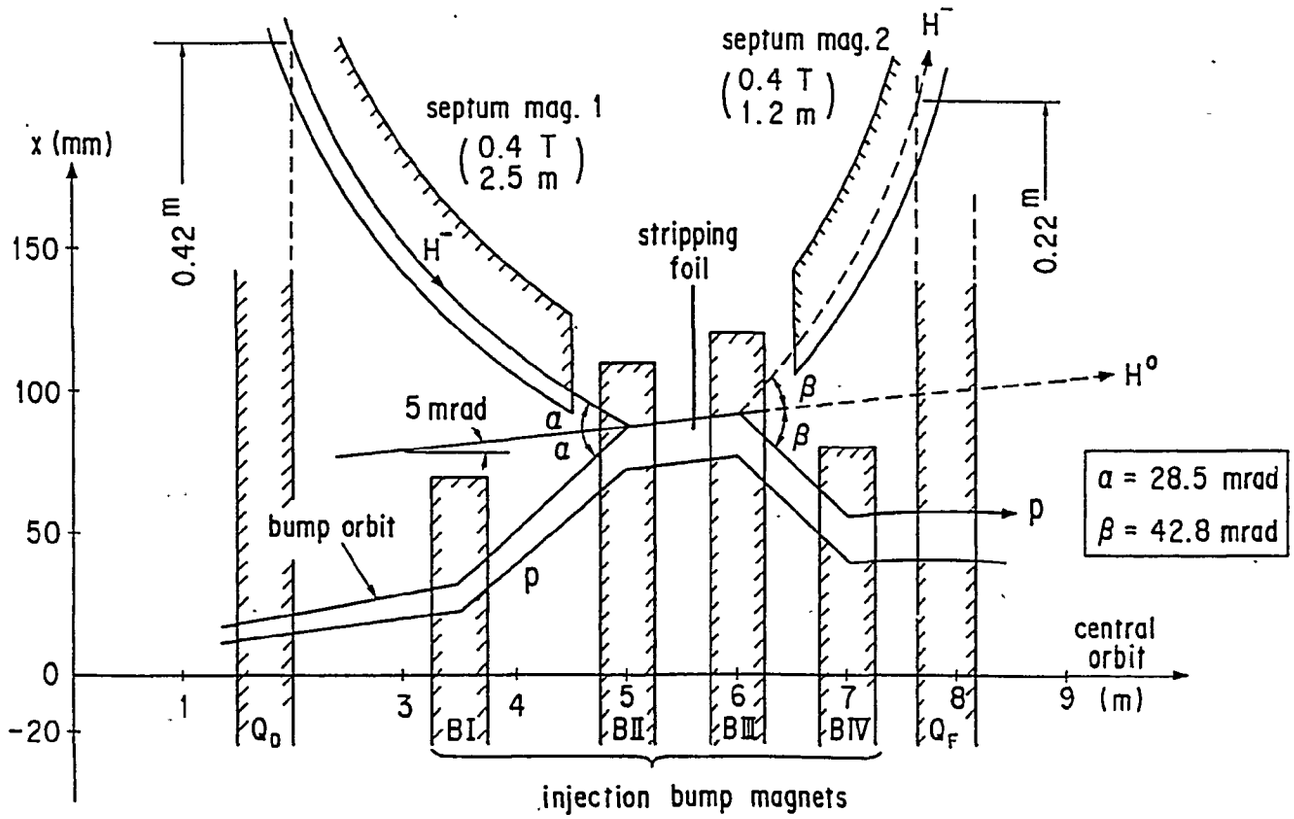

Fig. 19 Direct H^- injection : Case 1

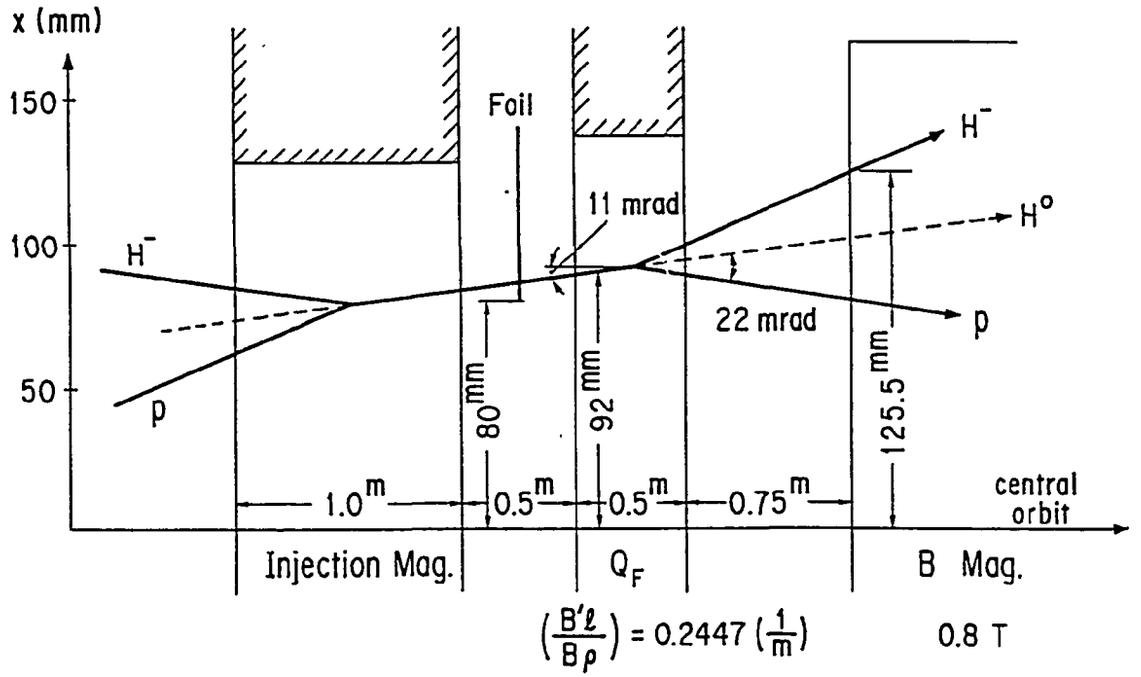

Fig. 20 Direct H^- injection : Case 2